POST-PROCESSING-BASED SOLAR PHOTOVOLTAIC DETECTION IN HIGH RESOLUTION AERIAL IMAGERY

Xuehua Guan[1], Wenwen Qi[1], Min Zhang[1], Ting Chen[1], Jianjun He[1,*], Qiang Wen[1], Zhiyong Wang[2].

[1] 21st Century Aerospace Technology Co., LTD., Beijing, 100096, China.

[2] Beijing Engineering Research Center of Small Satellite Remote Sensing Information, Beijing, 10096, China.

Email: hejj@21at.com.cn[1]

KEY WORDS: pixel-based classification, multi-feature classification and object-based classification

ABSTRACT: In recent decades, solar photovoltaic (PV) arrays constitute a significant portion of the rapidly increasing renewable energy systems. As a result, high quality information about PV, such as quantity, location, area and power capacity, has obtained substantial interest from the public. Existing imagery-based automatic PV arrays detection research are rare and accuracies are rather poor. In current PV arrays detection classifications, shadows and buildings are easily wrongly classified as PV arrays, due to their spectral similarity. In this context, our work presents a post-processing-based PV arrays automatic detection framework to further enhance the original classification accuracy. Firstly, automatic PV arrays detection is applied by a SVM classifier, and then a post-processing framework is designed to improve the original classification result. In detail, the post-processing framework is based on a two-level processing approach. In the first level, non-solar feature images are adopted to refine the classification commissions. In the second level, an objected-based approach is applied to decline the PV arrays boundaries. Experiments are evaluated by two high resolution aerial datasets, and results are further evaluated by the ground truth image from visual interpretation. And results underline the presented post-processing framework can effectively enhance the original classification accuracy.

1. INTRODUCTION

The emerging renewable energy systems, which provide environmentally friendly ways of producing resources, have got extensive attention from the worldwide. Specifically, solar photovoltaic (PV) arrays constitute a significant portion of the rapidly increasing renewable energy systems (Chersin et al, 2014). In spite of the PV arrays' small-scale size and scattered distribution, their environmental and economic benefits are stupendous. As a result, high quality information about PV arrays, such as quantity, location, area and power capacity, has obtained substantial interest from the government agencies, utilities, and decision makers and so on (Alam et al, 2014).

Although interests for the detailed information about PV arrays are expanding, it is nonetheless difficult to obtain. Traditional ways such as surveys and visual interpretations, are time consuming and inefficient (Malof et al, 2015). Fortunately, the emergency of the very high-resolution images which support for more detailed and accurate mapping, provides new avenues for the PV arrays detection task. However, very high spatial resolutions also pose challenges to image analysis as very high spatial resolution leads to high interclass spectral confusion (Huang and Zhang, 2009). As in very high resolution (0.12m) images, PV arrays usually appear in small-scale size objects and have serious spectral confusion with shadows and building roofs. Hence, there is an urgent demand to identify PV arrays from very high resolution images accurately.

Summarizing the existing literature, there are few studies reporting PV arrays detection via very high resolution images. One excellent work is the online public dataset of solar PV arrays (Bradbury et al, 2016), which contains over 19000 solar panels across 601 high-resolution images from four cities in California. However, all PV arrays of

This research was supported by the Beijing Municipal Science and Technology Commission (No. Z161100005016069).

Corresponding author: Jianjun He (E-mail address: hejj@21at.com.cn)

this dataset are manually annotated by MATLAB-based graphical user interface, while not by automatic detection means. Another pioneering study is the automatic detection of solar PV arrays via very high resolution images (Malof et al, 2015). In their study, rooftop images are firstly manually collected and then PV arrays are identified by automatic detection algorithm on each extracted rooftop image. Obviously, it is not a fully automatic PV arrays detection approach as it at first extracts rooftop images manually. However, both these two works are conducted by the same study group from Duke University, hardly have any other organizations published research results about PV arrays detection from very high resolution images.

Consequently, an advanced PV arrays detection approach which is not only automatic but also can identify PV arrays from the full image accurately is lacking. To meet with this requirement, we present an automatic PV arrays detection framework. An optimization strategy was carried out by post-processing-based approach to enhance the original classification result. The reminder of this paper is organized as follows. Section II describes the study sites and data sets. Section III presents the methodology of our work. Section IV describes the experimental results and analysis. Finally, section V concludes our work.

2. STUDY SITES AND EXPERIMENTAL SETTING

2.1 Study Sites

In this study, RGB images were obtained from the Google Earth (GE), which provides open, highly spatially resolved images suitable for information extraction task. And two typical areas of California are chosen for our study sites. One is the Firebaugh city, with its longitude and latitude ranging from W120°26′20″to W120°26′53″ and N36°50′20″to N36°50′49″, respectively. This study area not only scattered rooftop PV arrays but also distributed dense farm PV arrays. And the other is the building intensive city, named Hanford, whose geographic position is from W119°40′19″to W119°40′59″ and N36°20′31″to N36°21′3″, respectively. Both images are at a spatial resolution of 0.12m, and their projection is in the UTM Zone 48N system and Datum WGS 84. The overall images for these two cities and detailed images of PV arrays are shown in Figure 1.

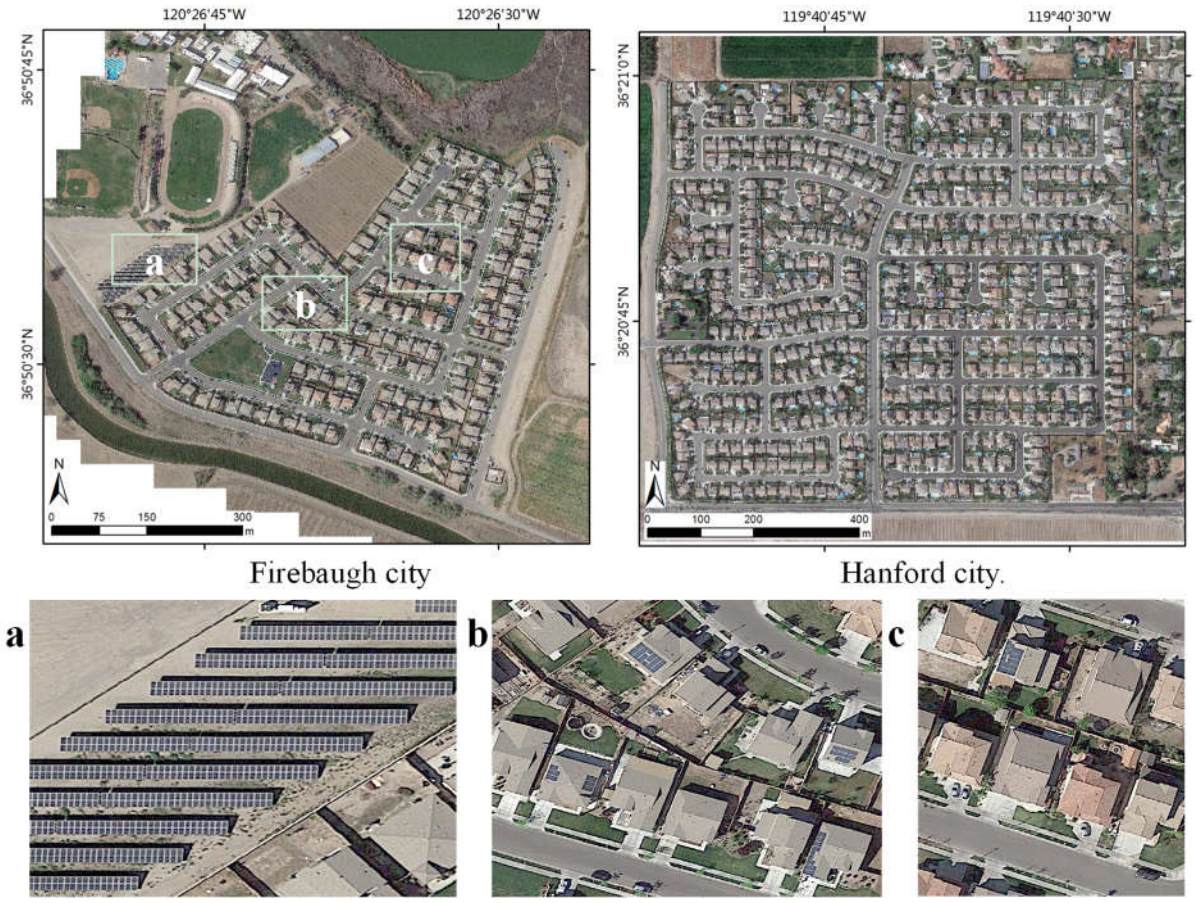

Figure 1 Study Areas, And Solar PV Detailed Images, Taking Firebaugh for Example.

2.2 Experimental Setting

All the classifications in our study are conducted by MATLAB platform. As the training dataset, we select positive and negative samples manually from the original RGB image, respectively. And the ground truth maps of the PV arrays are manually drawn beforehand using a polygon-based interaction tool. This ground truth map contains accurate information of the PV arrays distribution and is chiefly used in result verification. Numbers of training samples for these two data sets are list in the following table:

Table 1 Numbers of Training Samples

Class	Firebaugh	Hanford
Positive	1746	8827
Negative	6305	21971

To ensure the class diversity of training samples, in our pixel-based classifications all the training samples are applied to train classifier.

3. METHODOLOGY

3.1 The Proposed Classification Framework

Different from traditional high resolution classification problem, PV arrays detection is rather difficult, on account of their small-scale size and spectral-confusion with other classes. As a result, our work concentrates on the post-processing process to improve the initial poor detection accuracy. As is shown in Figure 2, our framework can

be achieved as follows: Firstly, a preprocessing procedure is applied on the input RGB image to remove shadows, as shadows exhibiting similar spectral characteristic with PV arrays. Followed by is a SVM classifier, which detects PV arrays by pixel-based classification. And at the same time, no-solar feature image is calculated from the RGB image to refine the pixel-based classification, generating the multi-feature classification result. Finally, a boundary image generated by multiresolution segmentation is adopted on the multi-feature classification map to decline the PV arrays' boundaries via objected-based approach. Accordingly, the proposed post-processing process approach includes the above multi-feature classification and the object-based classification.

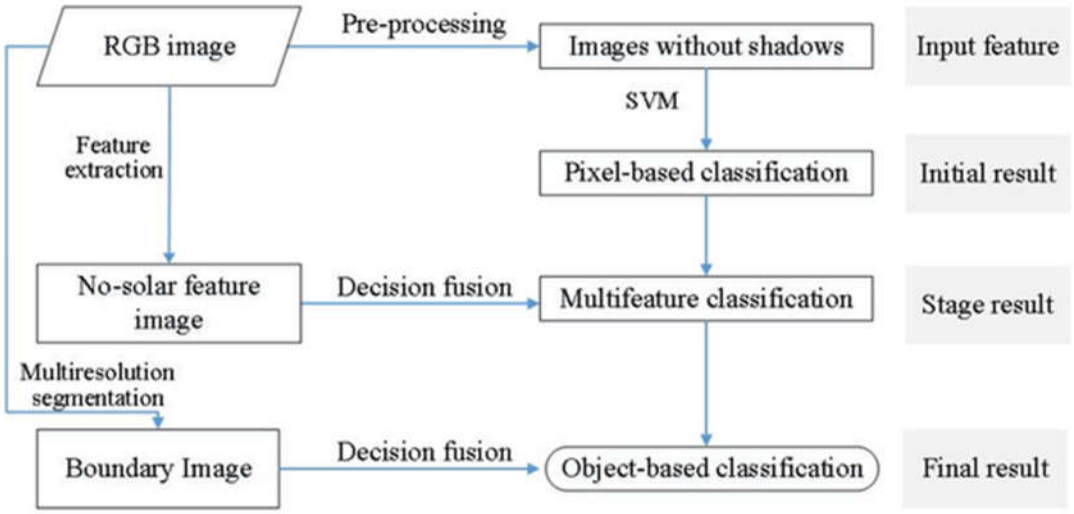

Figure 2 The Graphical Representation of the Overall Framework in This Article.

3.2 Pre-processing of Input Data Sets

Shadows, which are caused by height difference, exhibit confused spectral characteristic with land cover classes such as water and buildings in very high resolution images (Huang and Zhang, 2012). And for the PV arrays detection applications, the commission error caused by shadows are even significant. As a result, an effective shadow removal strategy is vital important for the precise detection of PV arrays. In this work, shadows are firstly removed from the input data sets by the commercial software eCognition according to layers brightness feature and object size difference. The rule of filtering of shadows from image can be expressed as follows:

For object(x)
IF $\text{brightness}_{\text{object}(x)}$ <T1 **AND** $\text{size}_{\text{object}(x)}$>T2
THEN object(x) is identified as shadow.
END

where T1 and T2 are set as 30 and 100, respectively. And object(x) denotes each object in the multiresolution segmentation image.

3.3 Pixel-based Classification

After pre-processing, images without shadows are put into classifier for pixel-based classification. Support vector machine (Fauvel et al, 2008) classifier is adopted in our study for all the classifications based on positive and negative samples, with *Penalty coefficient*=100, *kernel*=RBF (radial basis function), band width $\sigma=1/n$ (n is the dimension of the input features). And SVM classifications are conducted on the MATLAB platforms by LIBSVM toolbox (Chang and Lin, 2011).

3.4 Multi-features Classification

In our research, it is found that spectral profiles for PV arrays and buildings varying completely reversely from blue band to red band (Figure 3, Figure 4). Therefore, this spectral variation provides an excellent solution for the commission error caused by buildings. Based on this discovery, a feature map named non-solar feature image was developed by band match. The non-solar feature map is generated by a two-step process. Firstly, a grey image is calculated by subtracting red band using blue band. Then, a threshold is set on the grey image to get the non-solar feature image. Obviously, the non-solar feature image is a binary map, where pixels with values of 1 denote non-solar pixels and 0 values represent solar pixels. Accordingly, in order to deal with commission errors caused by spectral confusion between PV arrays and buildings, the non-solar feature image was regard as a constraint to refine the initial classification map in this work. And the multi-feature classification process can be expressed as follows:

For classification(x)
IF classification(x) = solar **AND** non-solar(x) =1
THEN classification(x) = unclassified
EDN

where classification(x) denote the value of each pixel in the pixel-based classification map, and non-solar(x) is the pixel value of each pixel in the non-solar feature image. Moreover, the x for classification(x) and non-solar(x) is the same pixel.

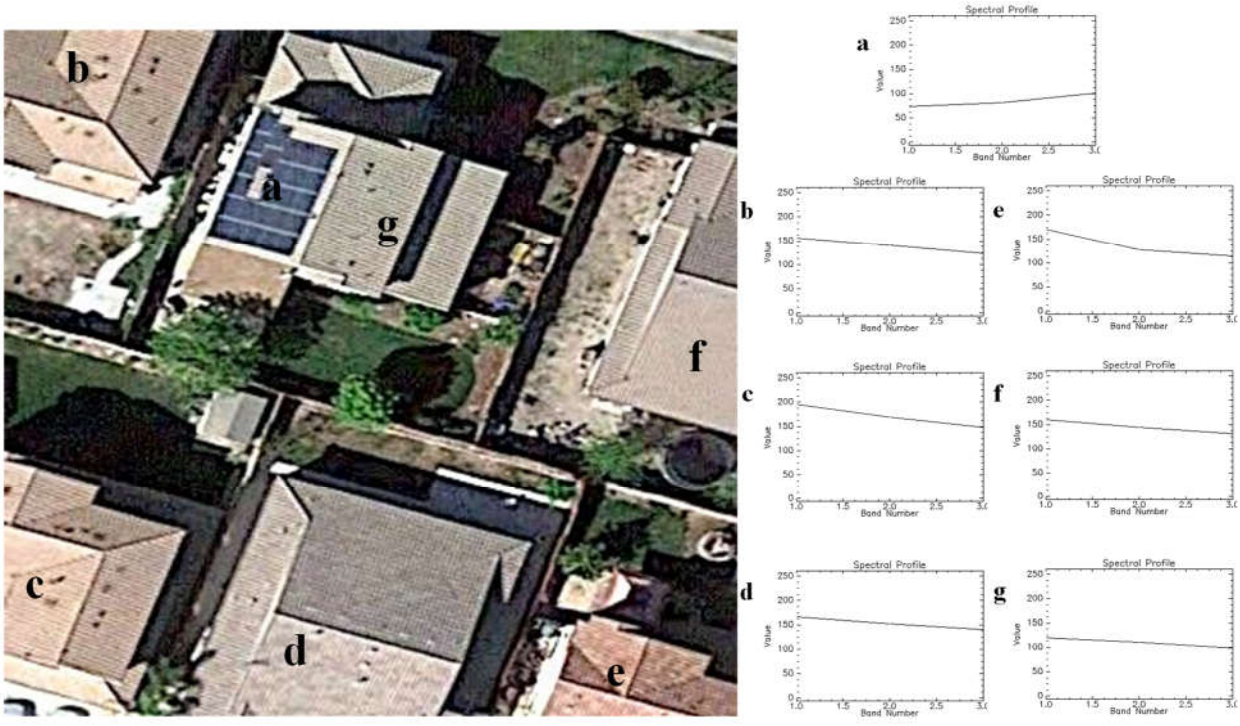

Figure 3 Spectral Curves for the PV Arrays and Surrounding Buildings, Taking Image Patch from Firebaugh for Example. And (a) Represents Spectral Curve of PV Arrays, while (b) ~ (g) Indicate Buildings' Spectral Curves.

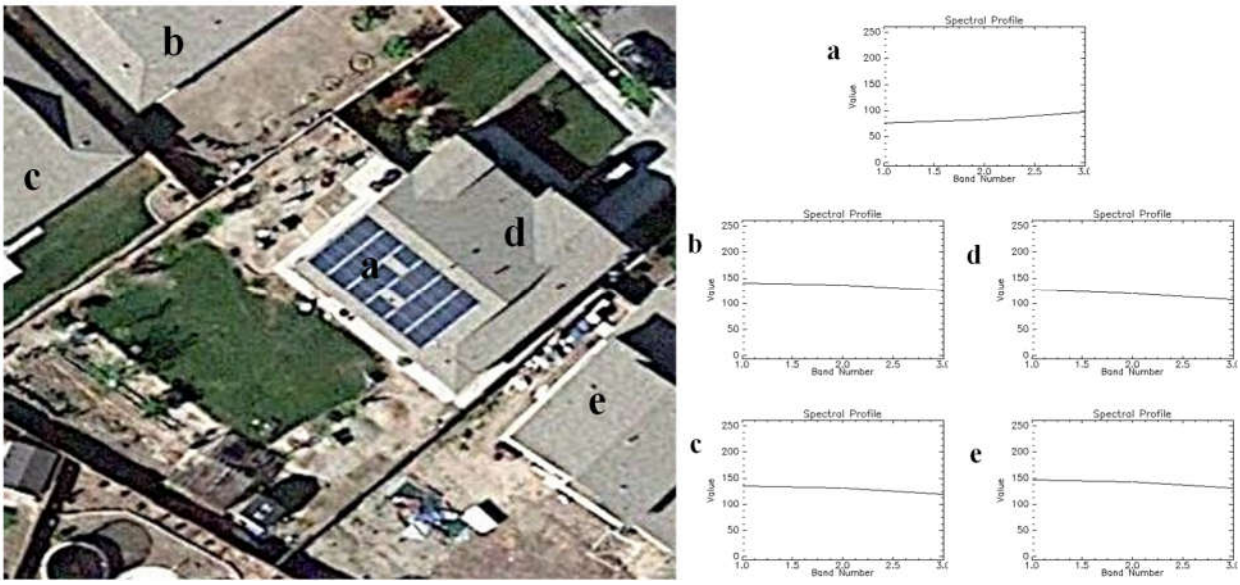

Figure 4 Spectral Curves for the PV Arrays and Surrounding Buildings, Taking Image Patch from Hanford for Example. And (a) Represents Spectral Curve of PV Arrays, while (b) ~ (e) Indicate Buildings' Spectral Curves.

3.5 Object-based Classification

The object-based classification proposed in our study aims at refining the PV arrays' shape, meanwhile, smoothing the noises on the exiting classification map (Aguilar et al, 2013). In this study, the object-based classification is to enhance multi-feature classification result by decision fusion with multiresolution image. Firstly, a multiresolution segmentation algorithm which is implemented in the commercial software eCognition, is adopted on the RGB image to acquire boundaries at different scales. And the segmentation criteria are set as follows: scale parameter is set to 30, with shape and compactness was set to 0.3 and 0.9, respectively. Afterwards, for the classification map generated by multi-feature classification, class labels for each object are relearned by majority voting according to the multiresolution image.

For object(x)

$\text{label}_{\text{object}(x)}$=Max_vote(label($x$))

END

where object(x) denotes each object in the segmentation image, and the label(x) represents the corresponding classification labels for object(x). Max_vote is to select the label that receives the largest votes for the object.

4. EXPERIMENTAL RESULTS AND ANALYSIS

PV arrays detection accuracies for each classification of these two study sites are reported in Table 2. It can be learned from the table that in spite of the high accuracies according to OA (Overall Accuracy), other accuracy index values such as KAPPA, PA (Producer Accuracy) and UA (User Accuracy) are rather poor. Since in practical applications, users usually perfect UA as a more objective accuracy evaluation index. Accordingly, in our study, we take UA as the accuracy index for experiment result comparison.

Regarding the PV arrays detection accuracies for Firebaugh, it can be seen from Table 2 that both multi-feature classification and object-based classification can improve the classification results significantly. And the best detection accuracies are obtained by object-based classification. The UA of Firebaugh increased from 0.06 to 0.47 when taking the post-processing procedure into account. However, when compared with Firebaugh, the accuracy increase for the Hanford city is not as evident, as UA improved by merely 0.17. This is because Hanford city

constitutes various PV arrays, which makes it difficult to identify due to their complex colors.

As it is shown in Figure 5 and Figure 6, the initial results are somewhat intriguing as classification maps displaying serious commission errors. When a careful analysis is done on the detailed detection maps, it can be learned that commission errors are removed from the initial class map step by step when the post-processing framework is applied. However, for the object-based classification, classification results are limited by the accuracy of multiresolution segmentation. As in the first line of Figure 5, some small size PV arrays are wrongly removed by the object-based classification process.

Table 2 Classification Accuracies for the Proposed PV Arrays Detection Framework.

City	Index	Pixel-based classification	Multi-feature classification	Object-based classification
Firebaugh	OA	0.97	0.93	0.99
	KAPPA	0.11	0.56	0.63
	PA	0.95	0.88	0.94
	UA	0.06	0.42	**0.47**
Hanford	OA	0.98	0.99	0.99
	KAPPA	0.17	0.30	0.39
	PA	0.70	0.65	0.72
	UA	0.10	0.21	**0.27**

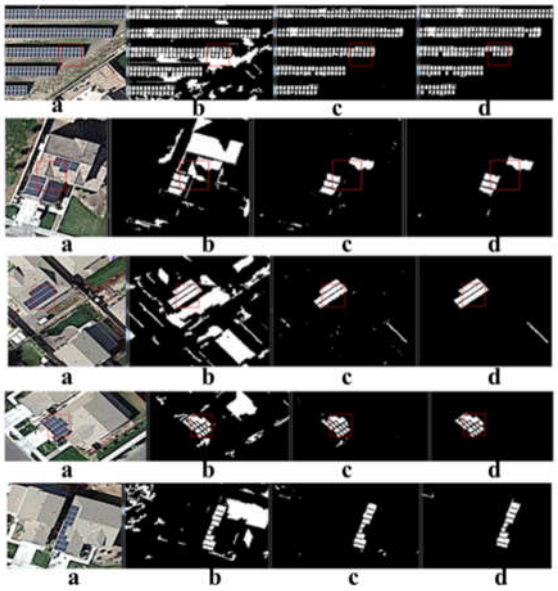

Figure 5 Detailed Result maps for PV Arrays Detection of Firebaugh: a. RGB Image; b. Pixel-based Classification Map; c. Multi-feature Classification Map; d. Object-based Classification Map.

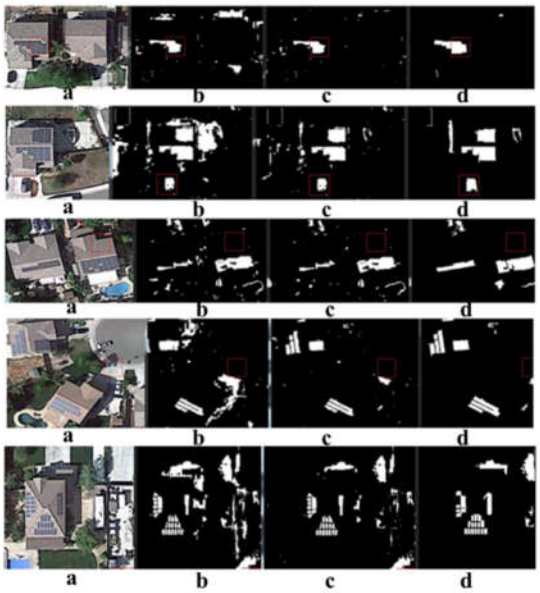

Figure 6 Detailed Result Maps for PV Arrays Detection of Firebaugh: a. RGB Image; b. Pixel-based Classification Map; c. Multi-feature Classification Map; d. Object-based Classification Map.

5. CONCLUSION

Detailed information about PV arrays is an essential parameter of renewable energy and plays a key role in urban planning and human behavior. However, at the present time, PV arrays information in the world is either lacking or incomplete for a number of countries. It is noting that the published PV arrays detection work cannot achieve automatic detection. To address this problem, in this study, we presented a fully automatic PV arrays detection approach. In the proposed framework, PV arrays are initially detected by SVM classification and were further optimized by the presented post-processing approach. Experiments which are undertaken on two Google images at 0.12m proved the effectiveness of our method. A more in-depth research, especially a more advanced and effective PV arrays detection framework will be investigated in our future work.

ACKNOWLEDGMENT

This research was supported by the Beijing Municipal Science and Technology Commission (No. Z161100005016 069).

REFERENCES

Aguilar, M. A., Saldaña, M. M. & Aguilar, F. J, 2013. GeoEye-1 and WorldView-2 pan-sharpened imagery for object-based classification in urban environments. International Journal of Remote Sensing 34, 2583–2606.

Alam M. J. E., Muttaqi K. M., and Sutanto D, 2014. An approach for online assessment of rooftop solar PV impacts on low-voltage distribution networks. IEEE Trans. Sustain. Energy. vol. 5, no. 2, pp. 663–672.

Bradbury K, Saboo R, Johnson T L, et al, 2016. Distributed solar photovoltaic array location and extent dataset for remote sensing object identification. Scientific data, 3: 160106.

Chang Chih-Chung and Lin Chih-Jen, 2011. LIBSVM : a library for support vector machines. ACM Transactions

on Intelligent Systems and Technology, 2:27:1--27:27. Software available at http://www.csie.ntu.edu.tw/~cjlin/libsvm.

Chersin A, Ongsakul W, Mitra J, Member S, 2014. Improving of Uncertain Power Generation of Rooftop Solar PV Using Battery Storage. Int. Conf. Util. Exhib. Green Energy Sustain. Dev., IEEE; 2014, p. 1–4.

Fauvel. M., Benediktsson. J. A., Chanussot J., and Sveinsson J. R., 2008. Spectral and spatial classification of hyperspectral data using SVMs and morphological profiles. IEEE Trans. Geosci. Remote Sens., vol. 46, no. 11, pp. 3804–3814.

Huang, X., and Zhang, L., 2009. A comparative study of spatial approaches for urban mapping using hyperspectral ROSIS images over Pavia City, northern Italy. International Journal of Remote Sensing, 30(12), pp. 3205-3221.

Huang, X., and Zhang L., 2012. Morphological Building/Shadow Index for Building Extraction from High-Resolution Imagery over Urban Areas. IEEE Journal of Selected Topics in Applied Earth Observations and Remote Sensing 5 (1), pp. 161–172.

Malof JM, Hou R, 2015. Collins LM, Bradbury K, Newell R. Automatic solar photovoltaic panel detection in satellite imagery. Int. Conf. Renew. Energy Res. Appl., IEEE, pp. 1428–31.

Yan, G., Mas, J. F., Maathuis, B. H. P., Xiangmin, Z., and Van Dijk, P. M. 2006. Comparison of pixel-based and object-oriented image classification approaches—a case study in a coal fire area, Wuda, Inner Mongolia, China. International Journal of Remote Sensing, 27(18), 4039-4055.